Agile quality-by-design development of alginate microparticles for encapsulation of hydrophilic drug

Asta-Ramaha Synthia Mackin-Mohamour, Julia Budzinski, Thierry Bastogne, Thibault Roques-Carmes, Veronique Sadtler, Philippe Marchal, Anne Sapin-Minet, Marianne Parent

Colloids and Surfaces A: Physicochemical and Engineering Aspects 693 (2024) 134053

Contents lists available at ScienceDirect

Colloids and Surfaces A: Physicochemical and Engineering Aspects

journal homepage: www.elsevier.com/locate/colsurfa

Agile quality-by-design development of alginate microparticles for encapsulation of hydrophilic drug

Asta-Ramaha Synthia Mackin-Mohamour [a,1,2], Julia Budzinski [b,2], Thierry Bastogne [b,c], Thibault Roques-Carmes [d], Veronique Sadtler [d], Philippe Marchal [d], Anne Sapin-Minet [a], Marianne Parent [a,*]

[a] Université de Lorraine, CITHEFOR, Nancy F-54000, France
[b] CYBERNANO, Nancy F-54500, France
[c] Université de Lorraine, CNRS, CRAN, Nancy F-54000, France
[d] Laboratoire Réactions Et Génie Des Procédés, Université de Lorraine, UMR 7274 CNRS, 1 rue Grandville, Nancy Cedex 54001, France

HIGHLIGHTS

- A QbD rational development of microparticles.
- Identification of critical parameters and impact assessment on particles CQA.
- Several regions respecting simultaneously the four specifications were found.

GRAPHICAL ABSTRACT

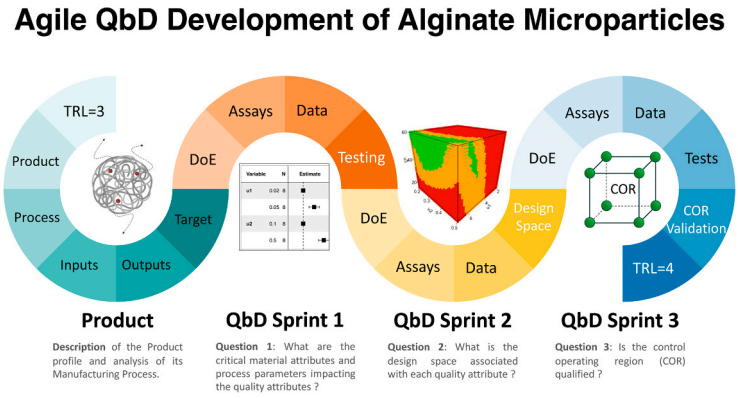

ARTICLE INFO

Keywords:
Quality-by-design
Microparticles
Alginate
Hydrophilic drug
Emulsion/ionotropic gelation

ABSTRACT

The development of alginate microparticles for encapsulation of hydrophilic drug is addressed. The alginate microparticles are produced by the emulsification/gelation process. The objective of this study is to optimize the encapsulation of sunset yellow, a model of small hydrophilic drug, by the means of an agile quality by design (QbD) approach. Five input factors are considered: the alginate concentration (2–7% w/V), the drug/polymer ratio (0.1/1–0.5/1), the cross-linker addition flow rate (1–1.6 mL/min), the cross-linker volume (5–10 mL), and the crosslinking time (15–60 min). Critical quality attributes (and their associated specifications) are the particle size ($\in [30; 150] \mu m$) and polydispersity, the encapsulation efficiency ($> 50\%$), and the drug loading ($> 10\%$). The implemented agile method follows three successive QbD sprints, each based on a specific design of experiments

* Correspondence to: EA 3452 CITHEFOR "Cibles thérapeutiques, formulation et expertise préclinique du médicament", Campus Brabois Santé, 9 avenue de la Forêt de Haye BP 20199, Vandoeuvre-Les-Nancy Cedex 54500, France.
E-mail address: marianne.parent@univ-lorraine.fr (M. Parent).
[1] present address: Univ. Lille, CHU Lille, ULR 7365 - GRITA - Groupe de Recherche sur les formes Injectables et les Technologies Associées, F-59000 Lille, France
[2] These both authors contributed equally to this work.

https://doi.org/10.1016/j.colsurfa.2024.134053
Received 17 January 2024; Received in revised form 18 April 2024; Accepted 21 April 2024
Available online 22 April 2024

(DoE). First, a screening of the process parameters is performed using a Plackett-Burman design, followed in a second sprint by the implementation of a central composite Hartley's design to identify the design space and to extract four eligible control operating regions where the probability to meet the CQA specifications is above 95%. In the last sprint, one of these optimal operating conditions has been qualified by testing eight end points of the region through the application of a full factorial design. This operating region corresponds to a combination of three factors: alginate concentration in [6.7;7]%, drug/polymer ratio in [0.29;0.34]w/w and a curing time in [40;60]min.

1. Introduction

Sodium alginate is a natural anionic polysaccharide widely used in the pharmaceutical, cosmetic and food industries [1]. It is an unbranched copolymer of L-guluronic acid (G) and D-mannuronic acid (M) randomly arranged and in various amounts, depending on the algae origin. In the presence of divalent cations such as calcium, alginate undergoes ionotropic gelation and forms a biodegradable gel which allows the encapsulation of active ingredients [2–5]. Depending on the formulation process, nano-, micro-particles or beads can be obtained, and the strength of the gel can be controlled through the concentration and properties of the polymer (*eg* molecular weight, composition in mannuronic acid (M) and guluronic acid (G) blocks: M/G ratio and sequence) as well as through the concentration of divalent cation [6]. Alginate can also be gelled through pH changes (at pH below the pKa of the uronic acids) [7], or desolvatation [8], or by chemical covalent cross-linking [9].

Due to its low cost, low toxicity, biocompatibility and biodegradability, alginate is one of the most studied polymers for controlled delivery of small drugs, macromolecules (proteins, enzymes, antigens) or even cells [10–15]. Moreover, alginate mucoadhesive properties increase the contact time between drug delivery systems and absorption sites, thus enhancing the bioavailability of the drug payload after buccal, nasal, pulmonary, vaginal or oral administration [16–20]. In this latter case, the pH-sensibility of the polymer matrix will also protect the drug against degradation by the gastric environment and enable a targeted release to the intestine [3,21]. Especially, oral delivery of hydrophilic drugs (peptides, proteins, nucleic acids…) might be achieved through encapsulation into suitable alginate carriers. The size of these carriers may vary from a few hundred nm for small nanoparticles up to several mm for large particles/beads, depending on their composition and process of fabrication.

The most popular methods used to produce alginate microparticles are spray drying, extrusion and emulsification/gelation [1,12]. In spray drying, a solution containing the polymer and the drug is pressurized and sprayed through a nozzle. The resulting mist is dried by hot gas in the drying chamber to form the microparticles. Due to the pressure and temperature stresses, this method is not suitable for fragile molecules. In extrusion process, the drug is added to the polymeric solution, and the resulting mixture is extruded into droplets to the hardening bath, containing the gelling agent. This technique is very simple, but produces rather large particles/millimeter-sized beads. An alternative method is emulsification/external gelation. In this case, the polymer-and-drug aqueous mixture (discontinuous phase) is emulsified into a large volume of oil (continuous phase). A surfactant is also added to stabilize the resulting water-in-oil emulsion. The gelling agent is finally added to the system to harden the emulsion droplets. Solid microparticles should then be separated and washed from the oily phase before use. This method is particularly suitable to encapsulate hydrophilic and fragile molecules by two aspects. Firstly, emulsification/ gelation does not induce thermal stress and secondly, the external oily phase limits the loss of the active ingredient from the hydrophilic matrix during microparticles formation. Furthermore, particle size can be tailored thanks to the emulsion process.

Quality by design (QbD) is a systematic approach of drug development widely used in pharmaceutical industry to shorten the time required for the development of new dosage forms and to develop a comprehensive understanding of the product and its manufacturing process [22]. In this approach, critical quality attributes (CQAs) of the drug product should be identified before using risk assessment tools such as Ishikawa diagram and Failure Modes and Effects Analysis matrices to identify and rank material attributes and process parameters with potential impact on product quality. An enhanced quality by design approach includes statistical techniques for the design of experiments (DoE) to establish an appropriate control strategy which can, for example, include a proposal for a design space, *i.e.* "the multidimensional combination and interaction of input variables (e.g., material attributes) and process parameters that have been demonstrated to provide assurance of quality" [22]. Working within this space is not considered as a change by the authorities: this regulatory flexibility might be highly advantageous for inevitable changes that may occur during the lifecycle of the product. Within this space limitations, the statistical model, determined from the experimental data, can predict the performance of formulations without preparing them.

QbD is also a growing trend in academic research for lipidic or polymeric formulations [23,24]. For example, some studies have conducted statistical comprehensive analysis of spray-drying [25] or extrusion process [26,27]. To our knowledge, despite its relevance to alginate particles production, the emulsification/gelation process has only been investigated in a single and recent study for optimization of isoniazid encapsulation efficiency and *in vitro* dissolution [28].

With the view of developing alginate microparticles encapsulating a fragile and hydrophilic active for mucosal delivery, the following CQAs may be considered: controlled particle size and size distribution, suitable encapsulation of the drug (expressed both as encapsulation efficiency and as drug loading, from an economic and a therapeutic point of view, respectively). In this study, CQA specifications have been set at [30–150 μm] for the particle size, with a narrow distribution if possible, $>$ 50% (w/w, drug encapsulated *versus* introduced) for drug encapsulation and $>$10% (w/w, drug encapsulated *versus* dried particles) for drug loading.

Drug release is also of interest, but was not considered in this study as it is partially dependent of particle size and drug loading and can be altered by subsequent modifications of particles, *e.g.* coating with other polymers. Several factors are likely to influence the properties of alginate microparticles (Fig. 1). Among them, and according to the literature, alginate concentration, external phase and surfactant, drug and cross-linker would be the most critical [12].

The aim of the present study was to determine the optimal formulation of alginate-based microparticles for hydrophilic drug encapsulation thanks to a rational quality-by-design approach. Most sodium alginate microparticle formulation processes are carried out in an aqueous dispersant phase, which can lead to premature leakage of the hydrophilic active ingredient during the manufacturing process, leading to weak encapsulation, or a burst effect during kinetic release of the drug. Here, microparticles were prepared with a modified emulsification/gelation process [10], in which the hydrophilic drug is confined in the aqueous droplets of the W/O emulsion, before being trapped in the microparticles produced by ionotropic gelation of the polymer by interactions with calcium ions. Despite its superiority for encapsulating hydrophilic drug, the emulsification/gelation process has not been extensively studied in the literature. In this study, an agile

implementation of Quality-by-design was applied to (i) screen the critical formulation factors, (ii) identify the design space and (iii) validate the optimal control operating region to synthetize microparticles suitable for mucosal administration of hydrophilic drug. We investigated the effect of various factors, such as alginate concentration, drug: polymer ratio, calcium chloride concentration and cross-linking time on the properties of the particles encapsulating sunset yellow, a model of small hydrophilic drug. We focus not only on drug encapsulation, but also on control of particles size, in order to gain a thorough knowledge about the impact of formulation and process parameters.

2. Materials and methods

2.1. Materials

The calcium chloride ($CaCl_2$), Span 80 as surfactant, Sunset Yellow (452 g/mol, solubility in water 19% w/v at room temperature, insoluble in oils) and sodium alginate (Alg-Na) powder (reference A1112, batch SCBX8356, viscosity = 8 cps for 1% in water at 25 °C, molecular weight range 30,000–100,000; experimental M/G ratio = 1.85) used were obtained from Sigma Aldrich (France). The fluid paraffin oil of pharmaceutical quality was supplied by COOPER (France). Organic solvents such as methanol (MetOH), ethanol (EtOH) and isopropanol (propan-2-ol) were purchased from Carlo ERBA Reagents (France). Phosphate Buffer Saline (PBS) (0.147 M, pH = 7.4) was prepared by using sodium phosphate (Na_2HPO_4), potassium phosphate (KH_2PO_4) and sodium chloride (NaCl) from VWR BDH® Chemicals (Germany) and potassium chloride (KCl) from Sigma Aldrich (Germany). The NaCl/sodium citrate solution (0.1 M / 0.1 M) was made using NaCl and sodium citrate from Sigma Aldrich (Austria).

2.2. Alginate sunset yellow microparticles formulation

An emulsification process was immediately combined with an ionotropic gelation process using calcium chloride as a cross-linker to obtain microparticles [10]. Alginate solutions of 2 and 5% (w/v) loaded with a model hydrophilic drug were prepared by dissolving sodium alginate and sunset yellow powder (drug concentration ranging from 10% to 50% (w/w of polymer) in deionized water and stirring until complete dissolution. The resulting aqueous solution was emulsified in paraffin oil containing 1% (v/v) surfactant (Span® 80) for 15 min at 20°C (aqueous/oil phases ratio of 1:10). The influence of the emulsification system (a paddle homogenizer (triple helix morphology, at 600 rpm, motor Heidolph RZR 2021, Germany) or an Ultraturrax®, (Ultraturrax® T25, Janke & Kunkel, IKA-Labortechnik, Germany) at 9500 rpm) was studied in exploratory experiments (see 2.4.1), and the paddle was selected for the following experiments. The emulsion droplets were cross-linked by standardized addition using a syringe pump (RAZEL® scientific instruments, United States) of a $CaCl_2$ solution (3% m/v) in isopropanol/methanol (3:2 v/v). Methods for adding the cross-linker (volumes, flow rates, curing time) were also explored as mentioned below. The suspension was then stirred for an additional 15 min and the resulting microparticles were recovered by filtration (Cellulose Nitrate Membrane Filters, 5.0 µm, Whatman). All material retained on the filter was washed three times with 15 mL of isopropanol to remove the residual external oily phase, before being spread in a glass dish and dried at 40°C in an oven with desiccant for 24 hours.

2.3. Physicochemical characterization of alginate microparticles

2.3.1. Particle size determination and size distribution

The dried microparticles were characterized according to their size and morphology by optical microscopy (Nikon Eclipse Ti, Japan, equipped with a Nikon camera and NIS-Elements F 3.0 imaging software). A few dried microparticles were re-suspended in isopropanol and observed under the optical microscope. Representative images of the sample were then analyzed one by one with the free software Image J (National Institutes of Health, USA). For each object identified, information such as area, perimeter and circularity values were automatically obtained and processed. The circularity was calculated with the formula: circularity = 4π*area/perimeter^2, the value varies between 0.0 for a very elongated object and 1.0 for a perfect circle. When the circularity reached values larger than or equal to 0.8, particles were considered as circular and their diameter was estimated accordingly. The particles "cut" by the edges of the photograph were not considered (no extrapolation). At least 100 isolated particles were analyzed for each condition. Due to the low number of particles measured, this protocol gives only an indication of their size, but has been shown to be reproducible between several operators. Light scattering was not suitable in this case, as the particles become transparent and tend to swell slightly when placed in water.

2.3.2. Drug loading and encapsulation efficiency

The encapsulation of sunset yellow was determined by extracting the drug from the dried microparticles in a NaCl (0.1 M)/sodium citrate (0.1 M) solution. As ionotropic gelation is a reversible phenomenon, chelation of calcium ions by sodium citrate leads to destruction of the microparticles, and the drug is released in the extraction medium. Thus, 10 mg of dried particles obtained in each condition were weighed and dissolved in 10 mL of extraction medium under magnetic stirring until complete disappearance of the particles. Then, 1 mL of the solution was recovered and centrifuged for 10 min at 10,000 rpm (MiniSpinplus Eppendorf, Germany). The supernatant was then collected and analyzed in a UV-Visible spectrophotometer (UV-2600 Shimadzu, Japan) at a

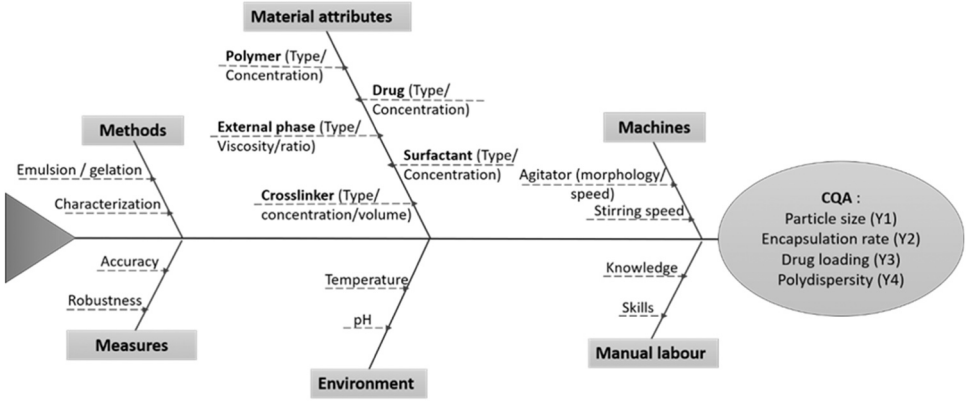

Fig. 1. Ishikawa diagram for evaluating risks in general, related to the quality of the alginate microparticles as hydrophilic drug delivery system. This diagram also allows us to identify a first input-process-output (IPO) model.

wavelength of 480 nm using a sunset yellow calibration curve.

Results were expressed as:

- Encapsulation efficiency EE = m_{DE} /m_{DT}
- Drug loading DL = m_{DE} /m_{MP}

Where m_{DE} and m_{DT} are the masses of the encapsulated and total drug used to produce the microparticles, and m_{MP} is the total mass of dried microparticles. Both expressions are traditionally used to characterize drug encapsulation: encapsulation efficiency reflects a performance of the process, while drug loading is more related to the therapeutic use (and is not affected by process yield).

2.4. Experimental designs and statistical analysis

2.4.1. Exploratory experiments

The stirring during emulsification and the surfactant concentration are two well-documented parameters impacting the size of emulsion droplets, and therefore the size of resulting particles [12,29]. To limit the parameters studied later in the DoE, they were varied in exploratory experiments, to set their values at optimum levels. Emulsification was performed either using a stirrer blade (at 600 rpm) or a homogenizer Ultraturrax® (at 9500 rpm). In parallel, a range from 0.2% to 2% (v/v) of Span® 80 was used to stabilize the W/O emulsion droplets [30]. The resulting droplets and particles were characterized.

2.4.2. Criticality assessment of four factors based on a Plackett-Burman design

A first set of experiments was designed according to a Plackett-Burman matrix that allows to estimate and rank the single effects of four different factors: the alginate concentration (u1), the drug/polymer ratio (u2), the crosslinker addition flow rate (u3), and the crosslinker volume (u4). The objective is to determine which of the four factors are critical process parameters (CPP). For the crosslinker, 5 or 10 mL of the $CaCl_2$ solution were used and the flow rate was 1 or 1.6 mL/min. The impact of these different factors u1 to u4 were explored by testing two levels, coded as low (-1) and high (+1) in Table 1. Namely, the responses were the mean particle size (Y1), the polydispersity (Y4), the encapsulation efficiency (Y2) and the drug loading (Y3). The statistical analysis used to analyze the effects of the four input factors on the four critical quality attributes relies on a linear regression applied to qualitative factors. A Student t-test was applied to all the regression coefficients. The criticality criterion of the factor effects consists in examining both their p-value and confidence interval [31]. The experimental design and the statistical analysis were performed in the R statistical computing environment.

2.4.3. Optimization of formulation using a central composite Hartley's design

For the process optimization, we kept the two most critical parameters previously identified, *i.e.* alginate concentration (u1) and drug/polymer ratio (u2), and we added a new factor: the crosslinking time (u5), not tested during the factor screening study since this process parameter was always known as critical. To establish the cause-effect relationship between these three critical process parameters and the three critical quality attributes: particles size (Y1), sunset yellow encapsulation efficiency (Y2) and loading (Y3), a central composite Hartley's design, given in Table 2, was implemented (the 3D representation of the design is given in Supplementary Data, Fig. A1). Each experimental condition was implemented in triplicate. Such a design is always associated with a surface response model structure, defined in (Eq. 1), which is particularly suitable for optimizing the response values and therefore identifying the best manufacturing conditions [32].

$$Y_k = \beta_0 + \sum_{i=1}^{3}\beta_i u_{i,k} + \sum_{i=1}^{2}\sum_{j=i+1}^{3}\beta_{ij} u_{i,k}u_{j,k} + \sum_{i=1}^{3}\beta_{ii} u_{i,k}^2 + \epsilon_k, \quad (1)$$

Table 1
Implemented Plackett-Burman design of experiments. Levels of the input factors are coded by −1/+1 to describe their low and high values respectively. The 8 trials were performed in duplicate in randomized order.

Codes	Independent factors	Level		units
		Low -1	High 1	
u1	Alginate concentration	2	5	% (w/v)
u2	Drug/polymer ratio	(0.1 / 1)	(0.5 / 1)	
u3	Crosslinker addition flow rate	1	1.6	mL/min
u4	Crosslinker volume	5	10	mL
	Dependent responses (critical quality attributes)			
Y1	Particle size			μm
Y2	Encapsulation efficiency (EE)			% (w/w)
Y3	Drug loading (DL)			% (w/w)
Y4	Polydispersity index			

	Experimental domain			
Trial order	**Alginate concentration (u1)**	**Drug/ polymer ratio (u2)**	**Crosslinker flow rate (u3)**	**Crosslinker volume (u4)**
1	-1	-1	-1	-1
2	1	1	-1	1
3	-1	-1	1	1
4	1	1	1	-1
5	1	-1	-1	1
6	-1	1	-1	-1
7	1	-1	1	-1
8	1	1	-1	1
9	-1	1	1	1
10	1	-1	-1	1
11	-1	-1	1	1
12	1	1	1	-1
13	-1	1	-1	-1
14	-1	1	1	1
15	1	-1	1	-1
16	-1	-1	-1	-1

with:

- k=1,…,n: is the index of the assay in the design of experiments;
- n: is the total number of experiments carried out;
- Y_k: value of the studied response variable Y for the k-th assay of the design;
- β_0: value of the mean response;
- β_i: additive effect of the i-th factor;
- β_{ii}: quadratic effect of the i-th factor;
- β_{ij}: interaction effect of the i-th and j-th factors on the studied response;
- $\epsilon_k \sim N(0,\sigma^2)$: modeling residual described by a random variable.

The coefficients of the model are estimated using the ordinary least squares method. The negligible effects are removed using backward stepwise selection based on the adjusted R^2 criterion. In the Quality by Design good practice, this data-driven modeling is also used to compute the design space, a set of input values, for which the probability for the responses (CQA) to meet the preset requirements is acceptable, *i.e.* greater than a given threshold often set at the value 0.95. Compared to usual response surfaces, the design space takes the modeling uncertainty (ϵ_k) into account and is therefore more adapted to risk assessment. To compute the design space, 4000 simulations of 27000 points uniformly distributed on the experimental domain were carried out. For each point, (i) we run 4000 simulations of a centered normal distribution with a standard deviation equal to $\widehat{\sigma}$, where $\widehat{\sigma}$ is the estimate of σ, the standard deviation of the modeling residuals; (ii) the response prediction, computed from the selected model, is added to the simulated modeling error; (iii) we count how many points among the 4000 simulations meet the specifications, (iv) the probability to meet the

Table 2
Coded variable description and values with the experimental domain for the Hartley's design. Each of the 11 trial was performed in triplicate.

Codes	Independent factors	Level values			units
		Low	Medium	High	
		-1	0	1	
u1	Alginate concentration	2	4.5	7	% (w/v)
u2	Drug/polymer ratio	(0.2 / 1)	(0.35/1)	(0.5 / 1)	
u5	Crosslinking time	15	37.5	60	min

	Experimental domain			
Trial	**Alginate concentration (u1)**	**Drug/polymer ratio (u2)**	**Crosslinking time (u5)**	**CQA (Specifications)**
F1	-1	-1	1	
F2	1	-1	-1	
F3	-1	1	-1	
F4	1	1	1	
F5	-1	0	0	**Y1:** Particle size (30–150 μm)
F6	1	0	0	**Y2:** EE (>50%)
F7	0	-1	0	**Y3:** DL (>10%)
F8	0	1	0	
F9	0	0	-1	
F10	0	0	1	
F11	0	0	0	

specifications is calculated (number of simulations fulfilling the specifications divided by the total number of simulations 4000). If this estimated probability is greater than 0.95, the point is in the design space represented in green, if it lies between 0.75 and 0.95, it belongs to a moderate risk region (orange), else it belongs to the Out Of Specification (OOS) region (red). The experimental design and the statistical analysis were performed in the R statistical computing environment.

2.4.4. Optimal formulation validation based on a 2^3 full factorial design

In the Quality by Design guidelines, the normal operating region (NOR) is defined by the European Medicine Agency as a region within the design space around the target operating conditions that contain common operational variability [33]. In this definition, common operational variability corresponds to uncontrolled variations. In this study, we wish to identify a region in which we can deliberately change values of the critical process parameters (CPP) while meeting the CQA specifications. To avoid any confusion with the NOR concept, we will use the term *control operating region* (COR) in this study. To validate the COR within the design space previously identified, a full factorial design was implemented. The eight experimental conditions of this design correspond to the eight corners of the COR *cube*. If those eight extreme operating conditions all meet the initial CQA specifications, the COR is considered as qualified. The validation full factorial design is described in Table 3.

3. Results and discussion

3.1. Experimental design: Exploratory experiments

In the emulsification/gelation process, both steps can impact particles size and drug encapsulation. As a result, a multitude of factors can influence the quality of the microparticles (Fig. 1). In a first approach, exploratory experiments were conducted to set parameters well known to control the stability and size of emulsion droplets [12,29]: the emulsification technique and the concentration of surfactant.

Firstly, shearing of the aqueous phase in the oily dispersing phase by the Ultraturrax was compared to the use of a triple helix blade. Ultraturrax generated very small globules compared to blade, resulting in particles too small to allow efficient separation by filtration (Fig. 2). It is well documented that higher energy input or increased stirring speed results in smaller droplets and then smaller particles. However, this larger interfacial surface area with the environment can lead to decreased encapsulation efficiency (as the drug might more easily diffuse into the oil phase) or faster drug release tendency from the resulting particles [12,29]. Consequently, the blade stirrer was used in further experiments.

Secondly, our study focused on the concentration of Span 80 used in the process. Span 80 is particularly suitable for W/O emulsions and dissolve well in liquid paraffin. Additionally, it is soluble in isopropanol so can be at least partially removed from the particles during washing. Surfactants play a crucial role in emulsification by reducing the interfacial tension between the two phases, and preventing resulting droplets from coalescence. In a previous study, Rastogi et al. [10] used 2% v/v of Span 80 in a similar protocol to encapsulate isoniazid in alginate microparticles. In this work, we tested different surfactant concentrations between 0.2% and 2% v/v (Fig. 3). In the literature, increasing Span 80 concentration generates significantly smaller emulsion droplets and consequently microparticles with smaller size and narrower distribution [34]. However, increasing surfactant concentration above a certain threshold can lead to reduced drug encapsulation [32]. Our results were consistent with these findings, as we found that yellow sunset encapsulation peaked for 1% of Span 80. At 2% of surfactant (corresponding to 100 times its critical micellar concentration in light paraffin [30]), we noticed that the oily phase after filtration of particles was yellow-colored, thus suggesting a massive micellar solubilization of the drug.

Therefore, the following formulations were made with the blade stirrer and 1% (v/v) of surfactant corresponding to an optimal encapsulation rate.

Table 3
Full factorial design 2^3 for validation with u1 = alginate concentration (%); u2 = drug/polymer ratio (w/w) and u5 = curing time (min). The 8 trials were performed once.

Trial N°	Alginate concentration (u1)	Drug/polymer ratio (u2)	Curing time (u5)
1	6.7	0.29	40
2	7	0.29	40
3	6.7	0.34	40
4	7	0.34	40
5	6.7	0.29	60
6	7	0.29	60
7	6.7	0.34	60
8	7	0.34	60

3.2. Criticality assessment of four input factors

Particles loaded with sunset yellow were produced by emulsion/gelation process. A Plackett-Burman design composed of eight different

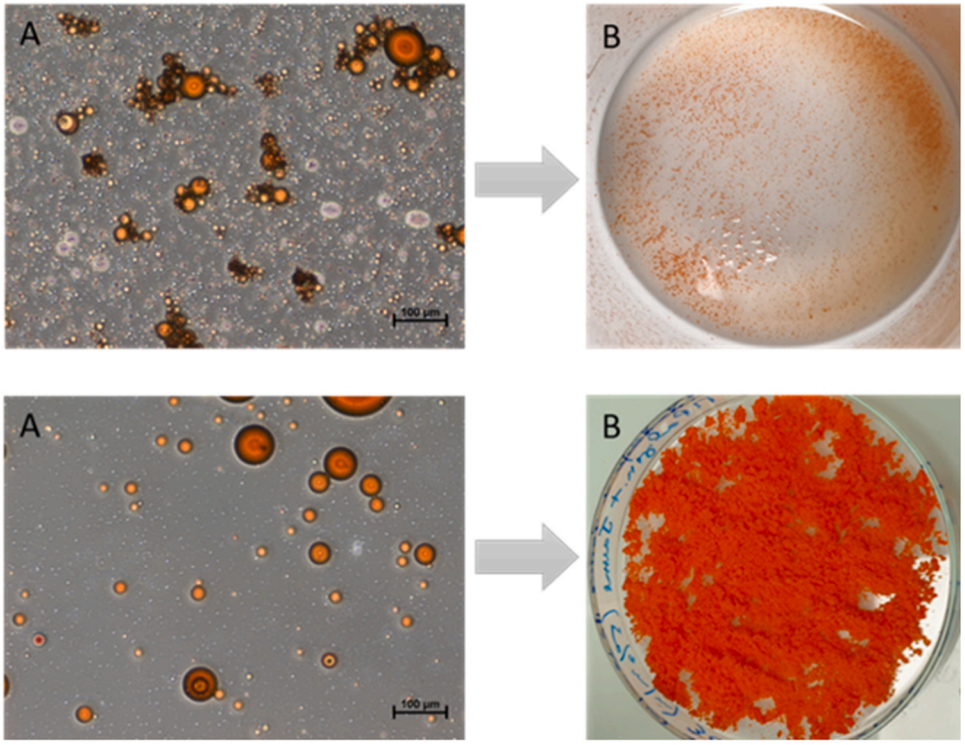

Fig. 2. Influence of shearing on emulsion droplets (A) and resulting particles recovery (B), with alginate solution at 5% w/v, drug concentration 20% (w/w polymer), 2% v/v of Span 80 in the paraffin phase and 5 mL of $CaCl_2$ solution added. Upper panel: 1 min Ultraturrax 9500 rpm and lower panel: 15 min triple helix blade 600 rpm. Scale bar is 100 µm.

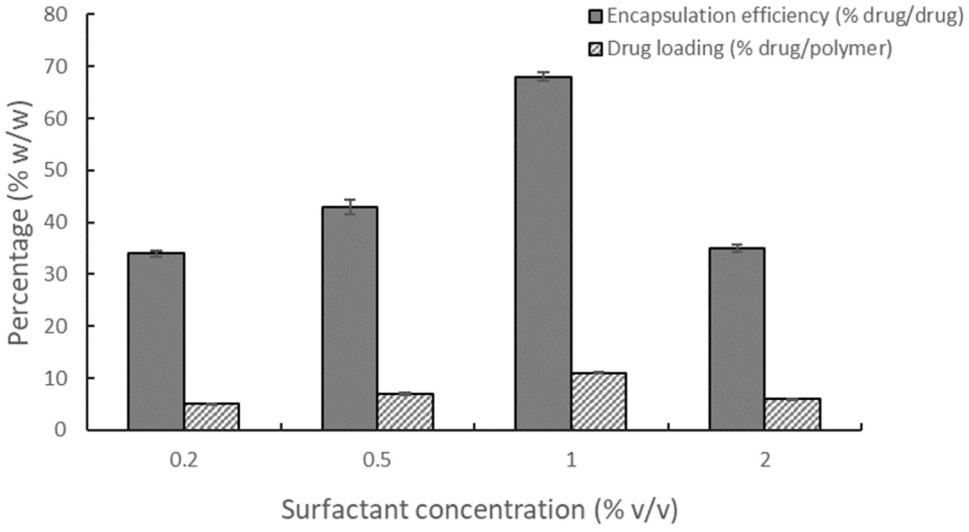

Fig. 3. Results of sunset yellow incorporation into microparticles formulated with alginate solution at 5% w/v, drug concentration 20% (w/w polymer) and 5 mL of CaCl2 solution added.

experimental conditions was carried out in duplicate and in randomized order to explore the impact of the alginate concentration (u1, at 2 or 5% w/v), the drug/polymer ratio (u2, at 10% or 50% (w/w polymer)), the crosslinker addition flow rate (u3, 1 or 1.6 mL/min) and the crosslinker volume (u4, 5 or 10 mL) on the particle size (Y1), the encapsulation efficiency (Y2), the drug loading (Y3) and the polydispersity (Y4) (Fig. 4).

Alginate concentration is widely recognized as a critical factor influencing microparticles morphology, size, and drug encapsulation. In the emulsification/gelation process, alginate concentration can be varied within a wide range, as viscosity of the alginate solution is not as limiting as in the extrusion process for example. Increasing the alginate concentration leads to increased viscosity of the alginate dispersion, thus higher interfacial tension between alginate droplets and the oil phase, higher interactions between alginate chains and calcium cations and finally larger microparticles (with wider polydispersity index). This higher internal space is generally associated with higher drug entrapment [12,29]. In our experiments, alginate concentration (u1) was indeed the most critical factor, impacting all four responses: the higher polymer concentration led to bigger particles, with better drug encapsulation but also a wider size distribution (Fig. 4). Aggregated particles were noticed only for 2% alginate. This is expected when the alginate

Fig. 4. Forest plots describing statistical results of the screening analysis (Plackett-Burman DoE). A: Effects of the four input factors on the particle size. B: Effects of the four input factors on the polydispersity. C: Effects of the four input factors on the encapsulation efficiency. D: Effects of the four input factors on the drug loading. u1= alginate concentration; u2= drug/polymer ratio; u3= crosslinker addition flow rate; u4= crosslinker volume. The forest plots allow to visualize and summarize the results of the linear regressions. For each factor, the first line corresponds to the reference modality of the factor and the second line to the second modality. Column « N » gives the number of observations for the studied modality. In the Plackett-Burman design, the number of observations is the same for all the modalities. The « estimate » column shows the estimation of the regression coefficient associated to a factor and its confidence interval at 95%. The details are given in the next column: the first value is the estimate of the mean effect on the response value and the values in bracket refers to the lower and upper bounds of the 95% confidence interval. The last value is the p-value of the student t-test on the regression coefficient. The results framed in red correspond to the process parameters estimated as critical.

concentration is too low, where clumping of small microparticles is classically observed (*eg* at 2% w/v for Rajinikanth et al. [35], no precision of alginate characteristics). As regards isolated particles, those with 5% of alginate had mean diameters around 40–100 μm while those with 2% of polymer were smaller (around 10 μm, Fig. 5). A similar trend was observed previously with FITC-BSA, with particles formulated with 4% of low viscosity alginate having 80–150 μm diameters *versus* 10 μm for those produced with 2% of the same polymer [36]. In our study, for both alginate concentrations, the particles were extremely polydisperse with a polydispersity index (PDI) of over 0.75. An encapsulation efficiency up to 80% was obtained in different conditions with a high drug loading above 10 mg for 100 mg of dried particles (from 10 to more than 50%) (Fig. 5). This result is stable when the particles are stored at 4–8 °C for at least 17 months (not shown). Whatever the preparation conditions, the particles fully release the active ingredient once placed in a physiological environment (see Figure A.2 in supplementary data).

Increasing the drug/polymer ratio (u2) from 10% to 50% (w/w polymer) led to slightly bigger particles, with improved sunset yellow encapsulation (both as encapsulation efficiency and drug loading). This result highlights the feasibility of a high drug content in our system, without overloading the capacity of microparticles.

Finally, the cross-linker volume (u4) had no significant effect on the four responses studied. One can therefore postulate that the calcium added, even at low volume, is sufficient to fully crosslink the available alginate chains. Interestingly, when the calcium is added with the faster flow rate (u3), drug loading and encapsulation efficiency are negatively impacted. In this case, calcium ions might diffuse quickly in alginate droplets and provoke a fast and intense gelification, thus contracting the polymeric chains and expulsing part of the drug outside the forming microparticles.

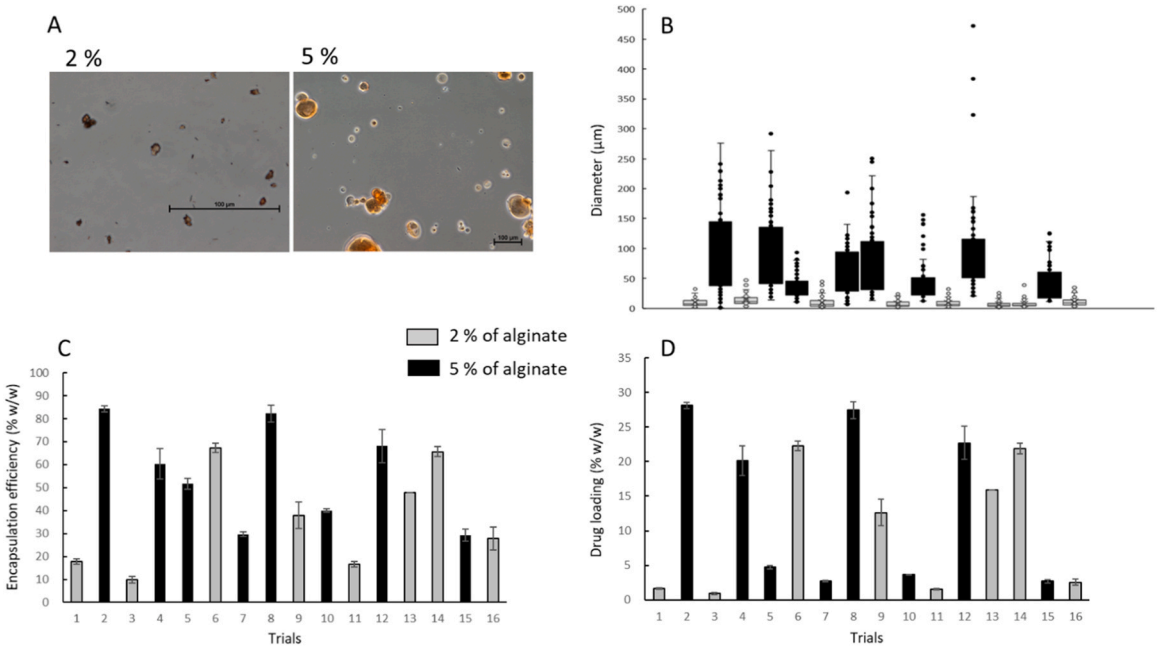

Fig. 5. Impact of alginate concentration (2 or 5%) on microparticles morphology (A, scale bars are 100 µm), size (B), encapsulation efficiency of sunset yellow (C) and drug loading (D).

In the following experiments, 10 mL of $CaCl_2$ were added at 1 mL/min, and the crosslinking time was varied. As none of the factors significantly reduced the polydispersity of particles, it was considered that this polydispersity is inherent to the stirring system [37] and this response was not be followed thereafter.

3.2.1. *Design space identification*

To determine the cause-effect relationships between the critical process parameters and the three response variables, a quadratic response surface model structure, presented in Eq. 1, is used to describe each CQA. Coefficients of each model are estimated from the experimental data collected after the application of the central composite Hartley's design presented in Section 2.4.3. Then, a design space and a control operating region are computed for each CQA. In the following, this method is successively applied to the response Y1, Y2 and Y3 (details of the statistics for each response surface model Y1, Y2 and Y3 are given in Supplementary data).

3.2.1.1. Control operating region for Y1. The response surface model of the particle size Y1, identified from experimental data, is as follows:

$$Y_{1,k} = -4.29 - 6.39u_{1,k} - 241.97u_{2,k} + 1.70u_{5,k} + 5.30u_{1,k}^2 + 454.93u_{2,k}^2 - 0.48u_{1,k}u_{5,k} + \epsilon_k, \quad (2)$$

with:

- k=1,…,n: is the index of the assay in the design of experiments;
- $\epsilon_k \sim N(0, \sigma^2)$: modeling residual described by a random variable.

The complete information about this model is reported in Table A1 of the Supporting Information. It appears that the coefficients of the quadratic effect of the parameter u_5 (β_{55}) and the coefficients of the interactions between u_1 and u_2 (β_{12}) and between u_2 and u_5 (β_{25}) can be neglected. The standard deviation of the modeling residuals is estimated to $\hat{\sigma} = 21.55$. The determination coefficient (R^2) of this model is 0.8688. This means that this model explains 86.88% of the variability of the data. Its adjusted R^2 is 0.8406.

In a second step, given the previously identified response surface model (Eq. 2), we carry out several numerical simulations and estimate the probability for each combination of CPP values (u1, u2, u5) of meeting the specification on Y1: 30 < Y1 < 150 µm. Fig. 6A plots all the estimated probabilities in the experimental domain. In this cube, the green region denotes the design space, *i.e.* a subspace of the experimental domain where the probability to meet the specifications for Y1 is greater than 95%. In the orange region, the probability falls between 75% and 95%. For the red region, the probability to meet the Y1 specification remains lower than 75%. Logically, only the design space is interesting and confirms that the objective on the particle size is achievable.

The last step consists in identifying the control operating region, *i.e.* a *cubic* area set in the design space and within which each process parameter (u1, u2, u5) can be modified independently from each other. Such a *cubic* area is not easy to represent in Fig. 6a. For Y1, the COR corresponds to alginate concentration u1 between 4.5 and 5.8, the ratio drug/polymer between 0.2 and 0.5 and the crosslinking time between 40 and 60 min. Note that these data are submitted for information purpose only since they are not validated by supplementary experiments.

3.2.1.2. Control operating region for Y2. The response surface model of the encapsulation efficiency Y2, identified from experimental data, is as follows:

$$Y_{2,k} \sim -86.07 + 45.19u_{1,k} + 119.68u_{2,k} + 0.66u_{5,k} - 3.87u_{1,k}^2 - 15.50u_{1,k}u_{2,k} + 0.11u_{1,k}u_{5,k} - 2.34u_{2,k}u_{5,k} + \epsilon_k, \quad (3)$$

with:

- k=1,…,n: is the index of the assay in the design of experiments;
- $\epsilon_k \sim N(0, \sigma^2)$: modeling residual described by a random variable.

The complete information about this model is reported in Table A2 of the Supporting Information. The terms β_{22} and β_{55} have been neglected by the estimation algorithm, meaning that u1 and u5 have no significant quadratic effects on Y2. The standard deviation of the modeling residuals is estimated to $\hat{\sigma} = 9.625$. The $R^2$of this model is equal to 0.8138. This means that the model explains 81.38% of the variability of

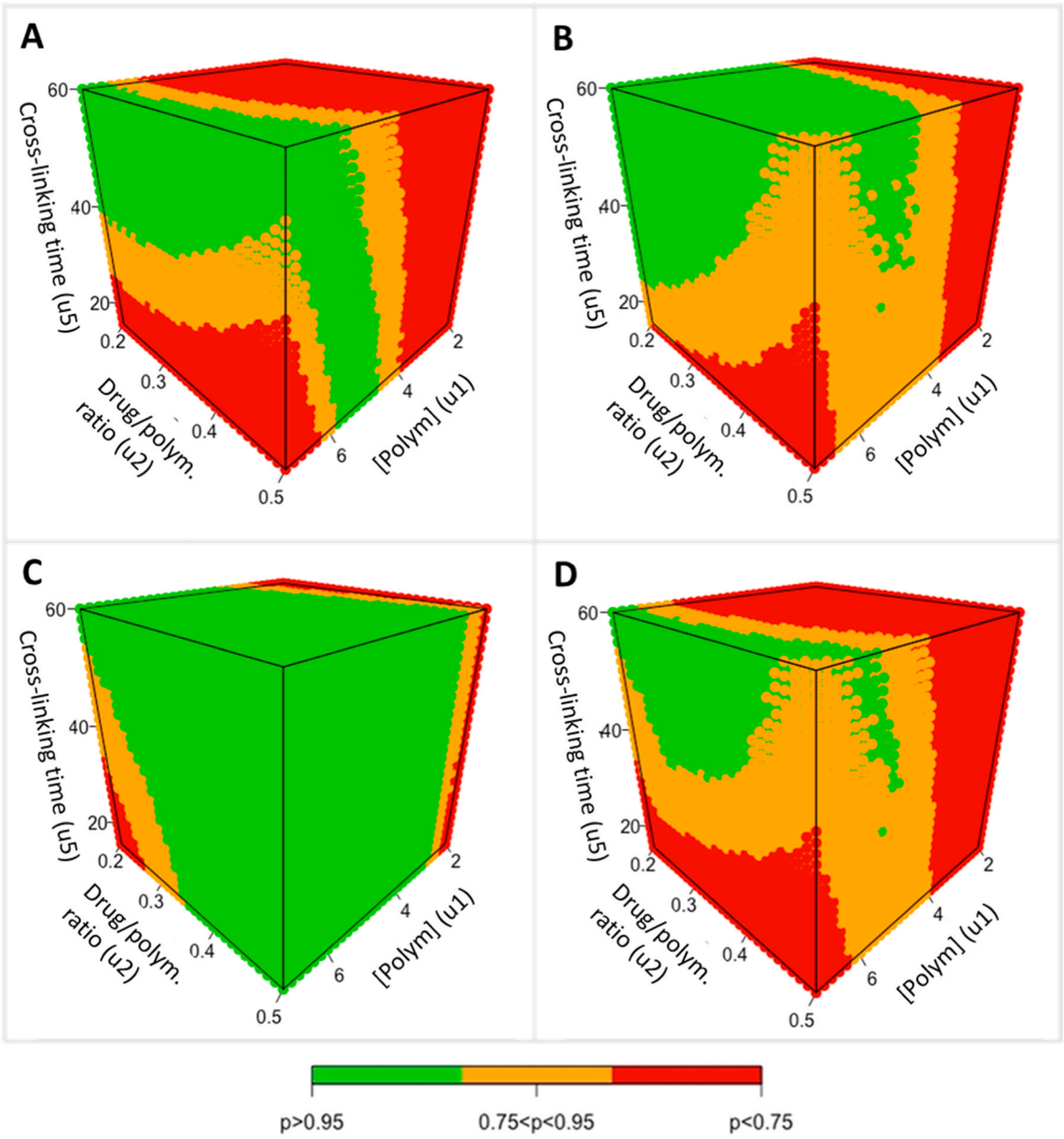

Fig. 6. Probability maps of three response variables **A**: particle size (Y1), **B**: encapsulation efficiency (Y2), **C**: drug loading (Y3) and **D**: the joint probability map related to the conjugate compliance of specifications on Y1, Y2 and Y3 (Table 2). Green regions correspond to the design spaces, i.e. a subset of factor values for which each specification has a probability greater than 95% to be met. In the orange regions, each response specification has a probability greater than 75% to be met. In the red region (Out-Of-Specification), the probability to meet the initial requirement is not acceptable, i.e. below 75%. u1=alginate concentration, u2=drug/polymer ratio and u5=cross-linking time.

the response variable Y2. Its adjusted R^2 is equal to 0.7655. The associated design space (green region) is relatively large. This emphasizes that an encapsulation efficiency above 50% is achievable. From this green design space, we have isolated a Control Operating Region in which the alginate concentration u1 can lie between 4.5 and 7, the ratio drug/polymer must stay in the range [0.2; 0.5] and the crosslinking time between 40 and 60 min (Fig. 6B). Note again that they are provided for the general guidance purpose only.

3.2.1.3. Control operating region for Y3. The identified response surface model of the drug loading Y3 is as follows:

$$Y_{3,k} \sim -28.64 + 10.79u_{1,k} + 40.10u_{2,k} + 0.21u_{5,k} - 0.97u_{1,k}^2 - 0.38u_{2,k}u_{5,k} + \epsilon_k, \quad (4)$$

with:

- k=1,…,n: is the index of the assay in the design of experiments;
- $\epsilon_k \sim N(0, \sigma^2)$: modeling residual described by a random variable.

The complete information about this model is reported in Table A3 of the Supporting Information. In this model, the quadratic effects of u2 and u5, the interaction between u1 and u2 and between u1 and u5 are neglected by the estimation algorithm. In other terms, according to the experimental data, there no quadratic effects of u2 and u5 but there is a significant interaction effect between u2 and u5. The standard deviation of the modeling residuals is estimated to: $\widehat{\sigma} = 2.81$. The R^2 of the model is 0.8223, while its adjusted R^2 is equal to 0.79.

Fig. 6C depicts the design space to obtain a drug loading larger than

10% with a probability greater than 95%. Within the design space, we have extracted a COR (cubic subspace) in which each factor can be changed independently from each other. For Y3, the polymer concentration needs to be larger than 2.5, the ratio of drug to polymer must be larger than 0.35 (or between 0.35 and 0.5), while the crosslinking time must be greater than 50 min (between 50 and 60 min).

3.2.1.4. Global control operating region. The final step consists in determining which combinations of the factors allow to meet all the CQA specifications: Y1, Y2 and Y3 with a probability greater than 95% for each one. The joint probability map is given in Fig. 6D. Regarding this obtained joint probability map, four control operating regions were identified: (i) $u_1 \in [6.55; 7.5], u_2 \in [0.26; 0.35] and u_5 \in [41, 55]$, (ii) $u_1 \in [6.55; 7]$, $u_2 \in [0.28; 0.35] and u_5 \in [41, 56]$, (iii) $u_1 \in [6.7; 7]$, $u_2 \in [0.29; 0.34] and u_5 \in [40, 60]$, and (iv) $u_1 \in [6.7; 7]$, $u_2 \in [0.29; 0.4] and u_5 \in [45, 60]$. Among these four possibilities, we have chosen to test the last Control Operating Region (iv) since it corresponds to the best practical and relevant compromise (weighing power, solubilization of the drug and limited experimentation time) for our future experiments.

3.3. Validation of a control operating region

This validation of a Control Operating Region (COR) is the last part required for the QbD method. It consists in checking there exists a subregion, often a cube, set within the design space in which all operating points lead to comply all the CQA specifications with an acceptable probability. Since it is impossible to test all the constitutive points of the COR, only the furthest points (corners of the cube) are evaluated, with experimental data different from those used previously to build the model. In this case, it consists in applying a 2^3 full factorial design. Fig. 7 shows the predicted values and their 95% confident interval compared with the experimental values for the 8 validation experiments. Details of the size distribution of the 8 batches for validation are given in Table A4 in supplementary data.

The experimental values always fall in the prediction range, except for 3 points among the 24. Nevertheless, in all cases, CQA specifications are met. However, particles were still slightly polydisperse but non-aggregated. Particle size real values were comparable to those expected by the model with a mean of the size between 100 μm and 125 μm for the real values against 70 μm to 110 μm for the expected values with 14 μm for the lower and 160 μm for the upper. Experimentally, the encapsulation efficiency reached more than 70% with a maximum drug loading of 19 mg of drug for 100 mg of dried particles. These values were similar than those expected which demonstrates the robustness of the model-based predictions.

QbD is a hot topic in pharmaceutical development for drug characterization [38–40] or formulation, whether for soft phases (liposomes [41]) semi-solids (gels [42]) and solid forms (tablets [43], particles [44]). A QbD rationale was applied to develop alginate microparticles for encapsulation and oral delivery of hydrophilic drugs. Several variables influencing microparticles performances were identified, providing an increased understanding of this emulsification/gelation process and assuring flexibility of formulation. As expected [12], the polymer concentration and the drug/polymer ratio were the most critical factors, although the introduction of cross-linking agent has also an influence.

Among the four control operating regions identified, one was validated, and the developed statistical models were able to predict the experimental results with an acceptable precision. A small, very hydrophilic and ionizable model drug was used for this study. It remains to be seen how easily these results can be transposed to other molecules of therapeutic interest. In this case, further characterization of the particles will be needed, *e.g. in vitro* release profile, depending on their

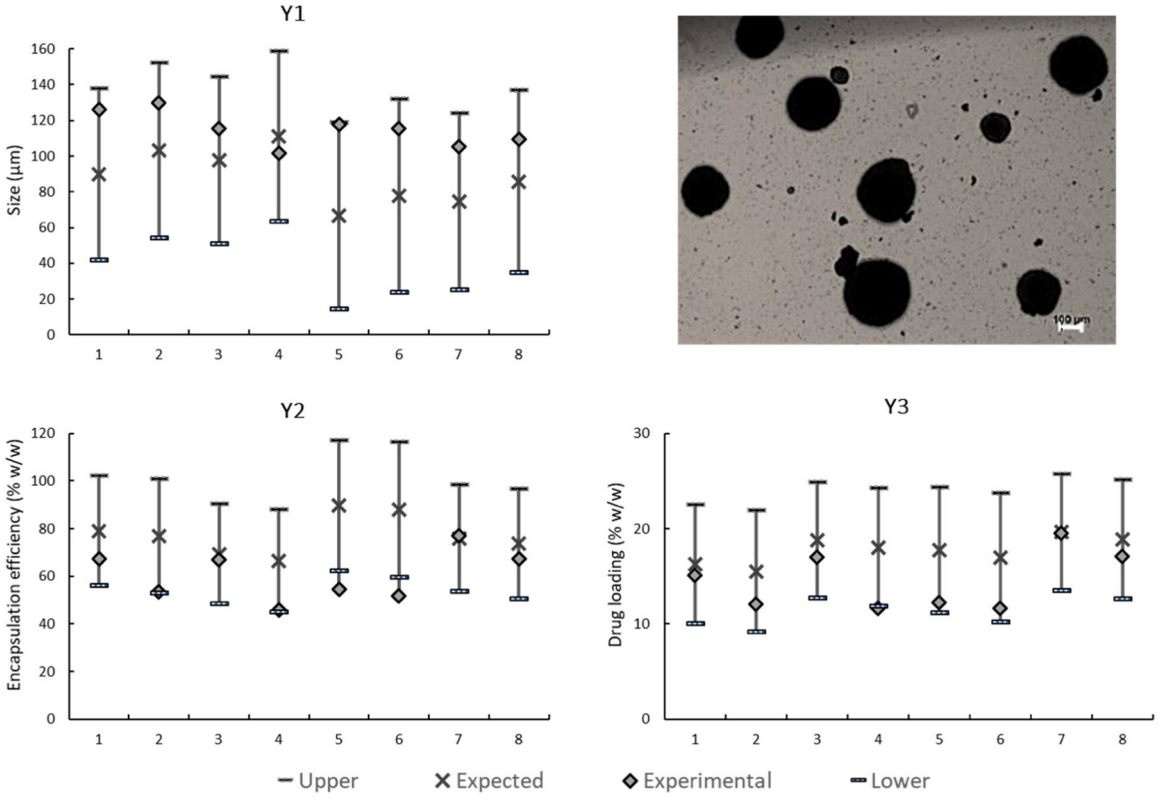

Fig. 7. Particle morphology observed in optical microscopy with 40 times magnification and critical quality attributes (Y1 = microparticles size, Y2 = encapsulation efficiency and Y3 = drug loading) expected and real values obtained for the 8 trials of the validation design with minimum and maximum value according to the prediction interval at 95%.

therapeutic applications.

4. Conclusions

The optimization of the encapsulation of hydrophilic drug by alginate microparticles was conducted using a QbD approach. The production of the microparticles was performed by the emulsification/gelation process for which the hydrophilic drug was confined inside the aqueous droplets of the W/O emulsion, before being trapped in the microparticles produced by ionotropic gelation of the alginate polymer by interactions with calcium ions.

The optimization of the hydrophilic sunset yellow encapsulation was performed following an agile QbD approach decomposed into three consecutive sprints, based each on different designs of experiments. In the first QbD sprint, four process parameters were screened using a Plackett-Burman design. The second sprint was devoted to identify the design space and control operating regions, i.e. ranges of the three critical process parameters in which the probability to meet the CQA specifications is above 95%. To this aim, a response surface model based on a central composite Hartley's design was computed. The last sprint used a full factorial design of experiments to quality one operating region.

After exploration experiments, factors selected were the alginate concentration, the drug to polymer ratio, the cross-linker addition flow rate and volume, and the cross-linking time. The tested alginate concentrations varied between 2% and 7% w/v. The drug to polymer ratios ranged between 0.1/1 and 0.5/1. The low level for crosslinker flow rates equaled 1 mL/min while the highest level read as 1.6 mL/min. The crosslinking volume was studied at 5 and 10 mL. The minimum cross-linking time was equal to 15 min while the maximum cross-linking time duration was 60 min. The critical quality attributes were the microparticles size and polydispersity, the encapsulation efficiency and the drug loading. The particle size had to be between 30 and 150 μm. The encapsulation efficiency was expected to be larger than 50% and the drug loading higher than 10%.

The results demonstrated that the CQAs specifications could be achieved for each response separately by a subtle combination of the values of the factors. For each response, the design space had a complex shape. The size of the control operating regions (COR) depended on the studied response. A large COR was obtained for the drug loading while smaller CORs were estimated for the particle size and encapsulation efficiency. More interestingly, we have identified a combination of the factors meeting the joint specifications of all CQAs with a probability above 95%. Four control operating regions were isolated. For the first region, alginate concentrations between 6.55% and 6.75%w/v, ratios of drug to polymer in the range 0.26 and 0.35, and crosslinking time between 41 and 55 min can be used. For the region 2, the alginate concentration was comprised between 6.55% and 7%w/v, the drug to polymer ratio ranged between 0.28 and 0.35, while the crosslinking time had to be between 41 and 56 min. For the third region, alginate concentrations between 6. and 7%w/v, ratios of drug to polymer in the range 0.29 and 0.34, and crosslinking time between 40 and 60 min were recommended. For the region 4, the alginate concentration was comprised between 6.7% and 7%w/v, the drug to polymer ratio ranged between 0.29 and 0.4, while the crosslinking time had to be between 45 and 60 min. Region 4 has been finally qualified after the application of 24 testing experiments.

In a future work, the optimal parameters found in this study will be used to encapsulate a more realistic active principle used in pharmaceutic with similar properties as sunset yellow. A thorough evaluation (size, encapsulation, release, stability) of these particles aimed at therapeutic applications will be conducted. In addition, the optimal parameters will be used to develop the same formulations using a microfluidic system in order to shift from a batch mode to a continuous mode.

Funding source

A.-R. S. Mackin-Mohamour's PhD was funded by the doctoral school of Biology Health and environment of « Université de Lorraine » and the French Ministry of Research. The authors also acknowledge support of EA 3452 by the "Impact Biomolecules" project of the "Lorraine Université d'Excellence" (Investissements d'avenir – ANR).

CRediT authorship contribution statement

Philippe Marchal: Writing – review & editing. **Véronique Sadtler:** Writing – review & editing. **Anne Sapin-Minet:** Writing – original draft, Supervision, Project administration. **Marianne Parent:** Writing – review & editing, Writing – original draft, Supervision, Project administration. **Thibault Roques-Carmes:** Writing – review & editing, Writing – original draft, Supervision. **Thierry Bastogne:** Writing – review & editing, Writing – original draft, Supervision, Methodology, Formal analysis. **Julia Budzinski:** Writing – original draft, Visualization, Software, Investigation. **Asta-Ramaha Synthia Mackin-Mohamour:** Writing – original draft, Visualization, Investigation.

Declaration of Competing Interest

The authors declare that they have no known competing financial interests or personal relationships that could have appeared to influence the work reported in this paper.

Data Availability

Data will be made available on request.

Acknowledgements

Authors thank Pr Sabine Bouguet-Bonnet and Dr Sebastien Leclerc from CRM^2, Université de Lorraine (UMR CNRS 7036), for the RMN characterization of alginate.

Appendix A. Supporting information

Supplementary data associated with this article can be found in the online version at doi:10.1016/j.colsurfa.2024.134053.

References

[1] A. Letocha, M. Miastkowska, E. Sikora, Preparation and characteristics of alginate microparticles for food, pharmaceutical and cosmetic applications, Polymers 14 (2022) 3834, https://doi.org/10.3390/polym14183834.
[2] K.Y. Lee, D.J. Mooney, Alginate: properties and biomedical applications, Prog. Polym. Sci. 37 (2012) 106–126, https://doi.org/10.1016/j.progpolymsci.2011.06.003.
[3] A.H.E. Machado, D. Lundberg, A.J. Ribeiro, F.J. Veiga, M.G. Miguel, B. Lindman, U. Olsson, Encapsulation of DNA in macroscopic and nanosized calcium alginate gel particles, Langmuir 29 (2013) 15926–15935, https://doi.org/10.1021/la4032927.
[4] L. Agüero, D. Zaldivar-Silva, L. Peña, M.L. Dias, Alginate microparticles as oral colon drug delivery device:a review, Carbohydr. Polym. 168 (2017) 32–43, https://doi.org/10.1016/j.carbpol.2017.03.033.
[5] J. Man, X. Wang, J. Li, X. Cui, Z. Hua, J. Li, Z. Mao, S. Zhang, Intravenous calcium alginate microspheres as drug delivery vehicles in acute kidney injury treatment, Micromachines 13 (2022) 538, https://doi.org/10.3390/mi13040538.
[6] M. Lopes, B. Abrahim, F. Veiga, R. Seiça, L.M. Cabral, P. Arnaud, J.C. Andrade, A. J. Ribeiro, Preparation methods and applications behind alginate-based particles, Expert Opin. Drug Deliv. 14 (2017) 769–782, https://doi.org/10.1080/17425247.2016.1214564.
[7] K.I. Draget, B.T. Stokke, Y. Yuguchi, H. Urakawa, K. Kajiwara, Small-angle X-ray scattering and rheological characterization of alginate gels. 3. Alginic acid gels, Biomacromolecules 4 (2003) 1661–1668, https://doi.org/10.1021/bm034105g.
[8] A. Maghsoudi, F. Yazdian, S. Shahmoradi, L. Ghaderi, M. Hemati, G. Amoabediny, Curcumin-loaded polysaccharide nanoparticles: optimization and anticariogenic activity against *Streptococcus mutans*, Mater. Sci. Eng. C. Mater. Biol. Appl. 75 (2017) 1259–1267, https://doi.org/10.1016/j.msec.2017.03.032.

[9] P. Sapuła P, K. Bialik-Wąs, K. Malarz, Are natural compounds a promising alternative to synthetic cross-linking agents in the preparation of hydrogels? Pharmaceutics 15 (2023) 253, https://doi.org/10.3390/pharmaceutics15010253.
[10] R. Rastogi, Y. Sultana, M. Aqil, A. Ali, S. Kumar, K. Chuttani, A.K. Mishra, Alginate microspheres of isoniazid for oral sustained drug delivery, Int. J. Pharm. 334 (2007) 71–77, https://doi.org/10.1016/j.ijpharm.2006.10.024.
[11] D. Dhamecha, R. Movsas, U. Sano, J.U. Menon, Applications of alginate microspheres in therapeutics delivery and cell culture: past, present and future, Int. J. Pharm. 569 (2019) 118627, https://doi.org/10.1016/j.ijpharm.2019.118627.
[12] N.Y.T. Uyen, Z.A.A. Hamid, N.X.T. Tram, N. Ahmad, Fabrication of alginate microspheres for drug delivery: a review, Int. J. Biol. Macromol. 153 (2020) 1035–1046, https://doi.org/10.1016/j.ijbiomac.2019.10.233.
[13] J.R. Lakkakula, P. Gujarathi, P. Pansare, S. Tripathi, A comprehensive review on alginate-based delivery systems for the delivery of chemotherapeutic agent: doxorubicin, Carbohydr. Polym. 259 (2021) 117696, https://doi.org/10.1016/j.carbpol.2021.117696.
[14] B. Reig-Vano, B. Tylkowski, X. Montané, M. Giamberini, Alginate-based hydrogels for cancer therapy and research, Int. J. Biol. Macromol. 170 (2021) 424–436, https://doi.org/10.1016/j.ijbiomac.2020.12.161.
[15] M. Xu, M. Qin, Y. Cheng, X. Niu, J. Kong, X. Zhang, D. Huang, H. Wang, Alginate microgels as delivery vehicles for cell-based therapies in tissue engineering and regenerative medicine, Carbohydr. Polym. 266 (2021) 118128, https://doi.org/10.1016/j.carbpol.2021.118128.
[16] O.C. Okeke, J.S. Boateng, Composite HPMC and sodium alginate based buccal formulations for nicotine replacement therapy, Int. J. Biol. Macromol. 91 (2016) 31–44, https://doi.org/10.1016/j.ijbiomac.2016.05.079.
[17] J. Lee, Y.M. Kim, J.H. Kim, C.W. Cho, J.W. Jeon, J.K. Park, L.H. Lee, B.G. Jung, B. J. Lee, Nasal delivery of chitosan/alginate nanoparticle encapsulated bee (*Apis mellifera*) venom promotes antibody production and viral clearance during porcine reproductive and respiratory syndrome virus infection by modulating T cell related responses, Vet. Immunol. Immunopathol. 200 (2018) 40–51, https://doi.org/10.1016/j.vetimm.2018.04.006.
[18] L. Gallo, V. Bucalá, M.V. Ramírez-Rigo, Formulation and characterization of polysaccharide microparticles for pulmonary delivery of sodium cromoglycate, AAPS PharmSciTech 18 (2017) 1634–1645, https://doi.org/10.1208/s12249-016-0633-9.
[19] B. Giordani, A. Abruzzo, U.M. Musazzi, F. Cilurzo, F.P. Nicoletta, F. Dalena, C. Parolin, B. Vitali, T. Cerchiara, B. Luppi, F. Bigucci, Freeze-dried matrices based on polyanion polymers for chlorhexidine local release in the buccal and vaginal cavities, J. Pharm. Sci. 108 (2019) 2447–2457, https://doi.org/10.1016/j.xphs.2019.02.026.
[20] Y.W. Zhang, L.L. Tu, Z. Tang, Q. Wang, G.L. Zheng, L.N. Yin, pH-sensitive chitosan-deoxycholic acid/alginate nanoparticles for oral insulin delivery, Pharm. Dev. Technol. 26 (2021) 943–952, https://doi.org/10.1080/10837450.2021.1966036.
[21] Y. Wang, J. Xuan, G. Zhao, D. Wang, N. Ying, J. Zhuang, Improving stability and oral bioavailability of hydroxycamptothecin *via* nanocrystals in microparticles (NCs/MPs) technology, Int. J. Pharm. 604 (2021) 120729, https://doi.org/10.1016/j.ijpharm.2021.120729.
[22] International Conference on Harmonization (ICH) Expert Working Group, ICH guideline Q8 (R2) on pharmaceutical development, ⟨http://www.ema.europa.eu/en/ich-q8-r2-pharmaceutical-development-scientific-guideline⟩, 2009 (accessed 12 June 2023).
[23] S. Cunha, C.P. Costa, J.N. Moreira, J.M. Sousa Lobo, A.C. Silva, Using the quality by design (QbD) approach to optimize formulations of lipid nanoparticles and nanoemulsions: a review, Nanomedicine 28 (2020) 102206, https://doi.org/10.1016/j.nano.2020.102206.
[24] G. Troiano, J. Nolan, D. Parsons, C. Van Geen Hoven, S. Zale, A quality by design approach to developing and manufacturing polymeric nanoparticle drug products, AAPS J. 18 (2016) 1354–1365, https://doi.org/10.1208/s12248-016-9969-z.
[25] H.I. Shahin, B.P. Vinjamuri, A.A. Mahmoud, R.N. Shamma, S.M. Mansour, H. O. Ammar, M.M. Ghorab, M.B. Chougule, L. Chablani, Design and evaluation of novel inhalable sildenafil citrate spray-dried microparticles for pulmonary arterial hypertension, J. Control. Release 302 (2019) 126–139, https://doi.org/10.1016/j.jconrel.2019.03.029.
[26] N. Mennini, S. Furlanetto, M. Cirri, P. Mura, Quality by design approach for developing chitosan-Ca-alginate microspheres for colon delivery of celecoxib-hydroxypropyl-β-cyclodextrin-PVP complex, Eur. J. Pharm. Biopharm. 80 (2012) 67–75, https://doi.org/10.1016/j.ejpb.2011.08.002.
[27] A. Mujtaba, M. Ali, K. Kohli, Formulation of extended release cefpodoxime proxetil chitosan-alginate beads using quality by design approach, Int. J. Biol. Macromol. 69 (2014) 420–429, https://doi.org/10.1016/j.ijbiomac.2014.05.066.
[28] D.R. Telange, R.R. Pandharinath, A.M. Pethe, S.P. Jain, P.L. Pingale, Calcium ion-sodium alginate-piperine-based microspheres: evidence of enhanced encapsulation efficiency, bio-adhesion, controlled delivery, and oral bioavailability of isoniazid, AAPS PharmSciTech 23 (2022) 99, https://doi.org/10.1208/s12249-022-02236-6.
[29] H. Choukaife, A.A. Doolaanea, M. Alfatama, Alginate nanoformulation: influence of process and selected variables, Pharmaceuticals 13 (2020) 335, https://doi.org/10.3390/ph13110335.
[30] E. Santini, L. Liggieri, L. Sacca, D. Clausse, F. Ravera, Interfacial rheology of Span 80 adsorbed layers at paraffin oil–water interface and correlation with the corresponding emulsion properties, Colloids Surf. A Physicochem. Eng. Asp. 309 (2007) 270–279, https://doi.org/10.1016/j.colsurfa.2006.11.041.
[31] J. Ranstam, Why the P-value culture is bad and confidence intervals a better alternative, Osteoarthr. Cartil. 20 (2012) 805–808, https://doi.org/10.1016/j.joca.2012.04.001.
[32] M.M. Ahmed, S.A. El-Rasoul, S.H. Auda, M.A. Ibrahim, Emulsification/internal gelation as a method for preparation of diclofenac sodium–sodium alginate microparticles, Saudi Pharm. J. 21 (2013) 61–69, https://doi.org/10.1016/j.jsps.2011.08.004.
[33] European Medicines Agency, Questions and answers: Improving the understanding of NORs, PARs, DSp and normal variability of process parameters. Technical report, EMA/CHMP/CVMP/QWP/354895/2017, ⟨https://www.ema.europa.eu/en/documents/scientific-guideline/questions-answers-improving-understanding-normal-operating-range-nor-proven-acceptable-range-par_en.pdf⟩, 2017 (accessed 3 July 2023).
[34] S. Mokhtari, S.M. Jafari, E. Assadpour, Development of a nutraceutical nano-delivery system through emulsification/internal gelation of alginate, Food Chem. 229 (2017) 286–295, https://doi.org/10.1016/j.foodchem.2017.02.071.
[35] P.S. Rajinikanth, C. Sankar, B. Mishra, Sodium alginate microspheres of metoprolol tartrate for intranasal systemic delivery: development and evaluation, Drug Deliv. 10 (2003) 21–28, https://doi.org/10.1080/713840323.
[36] E.N. Yaacob, J. Goethals, A. Bajek, K. Dierckens, P. Bossier, B.G. De Geest, D. Vanrompay, Preparation and characterization of alginate microparticles containing a model protein for oral administration in gnotobiotic european sea bass (*Dicentrarchus labrax*) larvae, Mar. Biotechnol. 19 (2017) 391–400, https://doi.org/10.1007/s10126-017-9758-4.
[37] E. Woo, H. Park, K.Y. Lee, Shear reversible cell/microsphere aggregate as an injectable for tissue regeneration: shear reversible cell/microsphere aggregate as an injectable for tissue regeneration, Macromol. Biosci. 14 (2014) 740–748, https://doi.org/10.1002/mabi.201300365.
[38] S. Dhiman, B.D. Kurmi, V. Asati, Analytical reversed-phase high-performance layer chromatography method development for silodosin and solifenacin in bulk and marketed formulation using analytical quality by design approach, Sep. Sci. 6 (2023) 2200117, https://doi.org/10.1002/sscp.202200117.
[39] G. Rajput, P. Patel, D. Singh, V. Asati, B.D. Kurmi, Quality by design assisted high-performance liquid chromatography parameters for simultaneous estimation of simvastatin and fenofibrate, Sep. Sci. 5 (2022) 566–578, https://doi.org/10.1002/sscp.202200078.
[40] S. Mondal, V. Asati, S.K. Verma, G.D. Gupta, B.D. Kurmi, P. Patel, Reversed-phase high-performance liquid chromatography analytical method development and validation for cefepime and sulbactam injection formulation assay: a quality by design approach, Sep. Sci. 6 (2023) e2200127, https://doi.org/10.1002/sscp.202200127.
[41] C.Y. Lee, C.T. Su, T. Tsai, C.M. Hsieh, K.Y. Hung, J.W. Huang, C.T. Chen, Formulation development of doxycycline-loaded lipid nanocarriers using microfluidics by QBD approach, J. Pharm. Sci. 112 (2023) 740–750, https://doi.org/10.1016/j.xphs.2022.09.023.
[42] D. Kesharwani, S. Das Paul, R. paliwal, T. Satapathy, Exploring potential of diacerin nanogel for topical application in arthritis: formulation development, QbD based optimization and pre-clinical evaluation, Colloids Surf. B Biointerfaces 223 (2023) 113160, https://doi.org/10.1016/j.colsurfb.2023.113160.
[43] S.K. Vemula, B. Daravath, M. Repka, Quality by design (QbD) approach to develop fast-dissolving tablets using melt-dispersion paired with surface-adsorption method: formulation and pharmacokinetics of flurbiprofen melt-dispersion granules, Drug Deliv. Transl. Res. 12 (2023) 3204–3222, https://doi.org/10.1007/s13346-023-01382-z.
[44] M.H.S. Dawoud, I.S. Mannaa, A. Abdel-Daim, N.M. Sweed, Integrating artificial intelligence with quality by design in the formulation of lecithin/chitosan nanoparticles of a poorly water-soluble drug, AAPS PharmSciTech 24 (2023) 169, https://doi.org/10.1208/s12249-023-02609-5.